Title

An Antigen-Delivery Protein Nanoparticle Combined with Anti-PD-1 Checkpoint Inhibitor Has Curative Efficacy in an Aggressive Melanoma Model

Journal

Advanced Therapeutics, 3(12)

ISSN

2366-3987

Authors

Neek, Medea
Tucker, Jo Anne
Butkovich, Nina
et al.

Publication Date

2020-12-01

DOI

10.1002/adtp.202000122

Peer reviewed

HHS Public Access

Author manuscript

Adv Ther (Weinh). Author manuscript; available in PMC 2021 December 01.

Published in final edited form as:

Adv Ther (Weinh). 2020 December ; 3(12): . doi:10.1002/adtp.202000122.

An Antigen-Delivery Protein Nanoparticle Combined with Anti-PD-1 Checkpoint Inhibitor Has Curative Efficacy in an Aggressive Melanoma Model

Dr. Medea Neek,
Department of Chemical and Biomolecular Engineering University of California Irvine, CA 92697, USA

Department of Chemical Engineering Stanford University Stanford, CA 94305, USA

Dr. Jo Anne Tucker,
Department of Medicine University of California Irvine, CA 92697, USA

Nina Butkovich,
Department of Chemical and Biomolecular Engineering University of California Irvine, CA 92697, USA

Edward L. Nelson [Prof.],
Department of Medicine University of California Irvine, CA 92697, USA

Chao Family Comprehensive Cancer Center University of California Irvine, CA 92697, USA

Institute for Immunology University of California Irvine, CA 92697, USA

Szu-Wen Wang [Prof.]
Department of Chemical and Biomolecular Engineering University of California Irvine, CA 92697, USA

Chao Family Comprehensive Cancer Center University of California Irvine, CA 92697, USA

Institute for Immunology University of California Irvine, CA 92697, USA

Department of Biomedical Engineering University of California Irvine, CA 92697, USA

Abstract

Immune checkpoint inhibition is a promising alternative treatment to standard chemotherapies; however, it fails to achieve long-term remission in a significant portion of patients. A previously developed protein nanoparticle-based platform (E2 nanoparticle) delivers cancer antigens to increase antigen-specific tumor responses. While prior work has focussed on prophylactic conditions, the objectives in this study are therapeutic. It is hypothesized that immune checkpoint inhibition, when augmented by antigen delivery using E2 nanoparticles containing CpG

wangsw@uci.edu.

Supporting Information
Supporting Information is available from the Wiley Online Library or from the author.

Conflict of Interest
The authors declare no conflict of interest.

oligonucleotide 1826 (CpG) and a glycoprotein 100 (gp100) melanoma antigen epitope (CpG-gp-E2), would synergistically elicit antitumor responses. To identify a regimen primed for obtaining effective treatment results, immune benchmarks in the spleen and tumor are examined. Conditions that lead to significant immune activation, including increases in gp100-specific interferon gamma (IFN-γ), CD8 T cells in the spleen, tumor-infiltrating CD8 T cells, and survival time are identified. Based on the findings, the resulting combination of CpG-gp-E2 and anti-programmed cell death protein 1 (anti-PD-1) treatment in tumor-challenged mice yield significantly increased long-term survival; more than 50% of the mice treated with combination therapy were tumor-free, compared with 0% and ≈5% for CpG-gp-E2 and anti-PD-1 alone, respectively. Evidence of a durable antitumor response is also observed upon tumor rechallenge, pointing to long-lasting immune memory.

Keywords

cancer vaccines; checkpoint inhibitors; combination therapies; nanoparticles

1. Introduction

One of the promising approaches in cancer immunotherapy is the blockade of immune checkpoint molecules,[1,2] which exist to support self-tolerance and immune system homeostasis, and to protect against autoimmunity.[3,4] Immune checkpoint inhibitors have demonstrated clinical efficacy in different advanced malignancies.[5,6] Despite favorable outcomes in some patients, however, treatments with checkpoint inhibitors are still not effective in a significant portion of patients, with only 20–40% of patients demonstrating long-term survival of 3 years post-treatment.[7–9] Immune checkpoint blockade enhances the existing immune reactivity (e.g., release the brakes on existing T cells) that may or may not be directed at specific tumor-associated antigens (TAAs). Thus, the efficacy could potentially be improved in the presence of higher and/or more specific antitumor T cell responses, such as those elicited by an antitumor vaccine. To examine this, different combination treatment strategies with immune checkpoint blockades have been under investigation.[10–12] We hypothesized that the combination of protein nanoparticle vaccines, to efficiently prime or educate the immune system, with immune checkpoint inhibitors would improve the antitumor efficacy in the aggressive, poorly immunogenic, B16-F10 tumor model.

Protein nanoparticle vaccines offer a number of advantages as antigen-delivery systems. Although conventional cancer vaccines (peptide- and protein-based vaccines) usually fail to efficiently elicit adequate immune responses against cancer cells,[13] the delivery of these peptides and proteins as components within nanoparticles has been shown to increase vaccine efficacy.[14] Various types of synthetic nano particles and virus-like vector systems have been evaluated as antigen-delivery platforms.[15–18] However, only a limited number of systems are in the optimal size range for lymphatic drainage and dendritic cell (DC) uptake (approximately 20–45 nm); such increased DC interactions result in more effective immune responses.[19] Our studies have focused specifically on protein nanoparticles whose attributes include their ideal size for vaccine delivery to lymph nodes and antigen-presenting

cells, highly organized structure and symmetry, and ability to be specifically functionalized.[15]

Our research group has been investigating the E2 protein-based nanoparticle (E2) for drug and antigen delivery.[20–25] Many protein nanoparticles are virus-like particles, but E2 has the advantage of being nonviral in source. The nanoparticle is derived from the E2 subunit of the pyruvate dehydrogenase complex from *Bacillus stearothermophilus*. It is self-assembled from 60 identical monomers that form a dodecahedral caged structure, and is very stable over a wide pH range and temperatures up to 80 °C.[26] E2 has a diameter of 25 nm, which is within the favored size range for lymphatic transport and DC uptake,[19] and it has an internal 12 nm hollow cavity that enables an internal location for molecular transport other than the outer surface.

Our lab has shown high efficacy of E2-based vaccines for multiple TAAs. We have previously demonstrated that the simultaneous delivery of CpG oligonucleotide 1826 (CpG) (adjuvant) and a major histocompatibility complex (MHC)-I restricted glycoprotein 100 epitope (gp100) (melanoma antigen) on E2 nano particles resulted in higher antigen-specific interfere on gamma (IFN-γ) secretion, compared to free-gp100 and free-CpG vaccines alone. This increase in IFN-γ secretion was associated with significantly delayed tumor development and prolonged median survival time with a prophylactic dosing regimen.[24] E2 nanoparticle vaccine efficacy was also studied in other tumor antigen models; significantly higher antigen-specific IFN-γ secretion and specific tumor cell lysis were achieved when one or more HLA-A2 restricted human cancer-testis antigens (NY-ESO-1, MAGE-A3) and CpG were simultaneously delivered by the E2 nanoparticle.[25] These investigations examined the broad protective and immunologic effects of the E2 vaccines, providing the foundation for development of a therapeutic vaccine strategy against pre-existing tumors in this current study.

Herein, we investigated the therapeutic effects after tumor challenge of E2-based nanoparticle vaccine alone, checkpoint blockade (anti-programmed cell death protein 1 (PD-1)) alone, and their combination. To determine effective conditions for eliciting antitumor responses, we tested different regimens of nanoparticle immunization and evaluated benchmarks such as T cell proliferation and tumor infiltration, PD-1 expression, tumor size, and survival. To our knowledge, our study is the first to test the combination of a protein-based nanoparticle vaccine with immune checkpoint inhibitors.

2. Results and Discussion

2.1. E2 Conjugated to CpG and gp100 Antigen Yielded Intact and Uniform Nanoparticles

Both CpG and $gp100_{25–33}$ were successfully conjugated to the internal cavity and surface of the E2 nanoparticle, respectively, to yield the vaccine (CpG-gp-E2) (Figure 1A). Consistent with prior syntheses,[10,11] the lower band on CpG-E2 at 28 kDa shows the unconjugated E2 monomer (lane b; Figure 1B), and the band at 35 kDa supports the conjugation of one CpG molecule (7 kDa) to an E2 monomer (lane c; Figure 1B). Simultaneous conjugation of CpG and gp100 to E2 nanoparticle resulted in two broad bands (lane d; Figure 1B), with the band between 35 and 40 kDa, confirming the simultaneous conjugation of gp100 and CpG to the

E2 monomers (CpG-gp-E2). The number of conjugated CpG and gp100 molecules per nanoparticle was quantified previously to be 22 ± 4 and 234 ± 36, respectively.[10] Also, dynamic light scattering revealed a hydrodynamic diameter of 27.8 ± 0.6, 27.6 ± 0.9, and 29.0 ± 0.9 nm for E2, CpG-E2, and CpG-gp-E2, respectively (Figure 1C); this size is important, as it is within the size range of 20–45 nm, which is reported to be optimal for nanoparticulate lymphatic drainage and dendritic cell uptake.[13] The zeta potentialsofE2,CpG-E2,andCpG-gp-E2nanoparticleswere−12.4±1, −11.3 ± 0.5, and −11.7 ± 1 mV, respectively, showing that conjugation of gp100 peptide and CpG to E2 nanoparticles did not change the overall surface charge. Our biodistribution studies of the E2 nanoparticles have shown that they are effectively taken up by almost 50% of DCs within the draining lymph nodes.[27] Because the surface charges of E2, CpG-E2, and CpG-gp-E2 nanoparticles are all similar, we expect no differences in uptake of these nanoparticles as a result of charge effects alone. Imaging with transmission electron microscopy (TEM) confirmed that the structure of nanoparticles remained intact after conjugation and that the size distribution was uniform (Figure 1D).

2.2. Establishing Optimal Treatment Schedule

It was unknown a priori what the optimal administration regimen for the combination treatment of anti-PD-1 and vaccine would be; such information depended on the immune responses and the tumor microenvironment (TME) after antigen exposure (e.g., PD-1 expression, IFN-γ secretion). Therefore, we examined the effects of different schedules of CpG-gp-E2 nanoparticle immunization to determine the most effective regimen for inducing antitumor responses against B16-F10 melanoma.

Mice were inoculated with 10^5 B16-F10 cells, followed by immunization with CpG-gp-E2 according to schedules depicted in Figure 2A. Group II received a single immunization of CpG-gpE2 on day 1, and Groups III and IV received a prime immunization of CpG-gp-E2 on day 1 followed by a booster 7 and 10 days after the prime immunization, respectively. ELISpot results and tumor size data on day 15 are presented in Figure 2B,C, respectively.

2.2.1. Single Immunization—A single immunization with 50 μg of CpG-gp-E2, which contains 5 μg of CpG and 5 μg of gp100 epitope (Group II, Figure 2A), resulted in a negligible amount of IFN-γ secretion from splenocytes on day 15 (Figure 2B). In our previous work, high frequencies of gp100-specific IFN-γ secretion after a single immunization of CpG-gp-E2 were observed in splenocytes after 7 days.[24] This suggests that the migration of antigen-specific IFN-γ producing (likely cytotoxic) T cells to the target site has occurred by 15 days, consistent with timing that has previously been reported in models of virus infections, other anti-tumor vaccine strategies,[28] and adoptive cellular therapy.[29] Although another possibility could be the induction of $FoxP3^+$ CD4 T cells, which can cause T cell suppression,[30,31] this is not a likely explanation because we did not detect an increase in the percentage of $FoxP3^+$ CD4 T cells (Figure S1, Supporting Information).

2.2.2. Double Immunization—Prime immunization of 50 μg of CpG-gp-E2 nanoparticle on day 1 followed by a booster on day 8 (Group III, Figure 2A) resulted in the

highest antigen-specific IFN-γ secretion (Figure 2B) and an enhanced antitumor response (Figure 2C) compared to other groups. Negligible levels of IFN-γ were observed for the splenocytes pulsed with an irrelevant peptide (SIINFEKL) (Figure 2B), confirming that the response was antigen-specific and not due to the E2 delivery platform itself. This specificity is consistent with our previously published work on cancer-testis antigens (NY-ESO-1 and MAGE-A3), which also demonstrated the antitumor responses to be confined toward the tumor antigens attached to the nanoparticle; we observed no IFN-γ response nor antigen-specific cell lysis against the irrelevant peptide or the tumor cells that did not express the antigen, respectively.[25] Comparison of Group III results with those of Group II suggests that a booster immunization is needed to induce a stronger therapeutic response.

Booster immunization 10 days after the prime immunization (Group IV, Figure 2A) resulted in a significantly lower amount of IFN-γ secretion compared to Group III ($p < 0.0001$) (Figure 2B). The difference in IFN-γ levels between Groups III and IV is likely due to kinetics of T cell activation. IFN-γ ELISpot analysis was performed on day 15, which is 4 days after the booster immunization in Group IV. The low level of IFN-γ secretion in Group IV suggests that T cells require more than 4 days after immunization to be activated. In contrast, the high levels of IFN-γ that was detected 7 days after booster immunization in Group III support strong T cell activation. Therefore, these data suggest that T cell activation for this vaccine occurs between 4 and 7 days after booster immunization. This kinetic is similar to a study of poly(lactic-*co*-glycolic acid) (PLGA) nanoparticles that reported peak T cell activation on day 5 following antigen delivery.[32]

Other comparable nanoparticle vaccine studies include the formulation of a gp100 epitope within a heat-shock protein (HSP)[33] and delivery of melanoma-specific TAAs using polymeric and liposomal nanoparticles.[34,35] However, one difference in our *in vivo* tumor challenge study to the HSP and PLGA therapeutic studies is our double-immunization schedule, resulting in more efficacy with fewer boosts than these other nanoparticle platforms.

2.3. A Significant Increase in CD8 T Cells Was Observed inSpleens of Mice That Received Double Immunization of CpG-gp-E2

It is well accepted that cytotoxic CD8 T cells have a preeminent role in identifying and destroying cancer cells.[36,37] Therefore, we examined how immunization with CpG-gp-E2 following each regimen (Figure 2A) affected T cell proliferation. Our data confirmed that T cell populations expanded in the splenocytes isolated from mice that received the double immunizations of CpG-gp-E2 nanoparticle (Groups III and IV).

Spleens isolated from Group III were larger in size compared to the phosphate buffered saline (PBS) control (Group I) (Figure 3A), which we interpret as an indication of generalized lymphocyte proliferation.[38] Splenocytes were examined to quantify CD4 and CD8 T cells, and representative flow data of CD8 T cells ($CD3^+CD8^+$) are presented in Figure 3B. Groups III and IV revealed an increase in both CD8 (Figure 3E) and CD4 T cells (Figure 3F), although the overall percentage of these cell types within the spleen did not change significantly (Figure 3C,D). We observed approximately 2× CD8 T cells in spleens isolated from Group III compared to the PBS control ($p < 0.0001$) (Figure 3E), and

approximately 1.6× CD8 T cells in Group IV relative to the control ($p < 0.05$) (Figure 3E). Relative to Group II (single immunization), 1.7× ($p < 0.001$) and 1.2× ($p < 0.05$) CD8 T cells were detected from Groups III and IV (double immunization), which supports the benefit of a booster injection (Figure 3E,F).

Furthermore, the higher CD4 counts observed in Groups III and IV, compared to the PBS control (Group I) (Figure 3F), did not correspond to an increase in the percentage of $FoxP3^+$ cells (Figure S1, Supporting Information). This suggests that the increase in the CD4 population was not due to an increased fraction of regulatory T cells (which can suppress immune responses), but likely T helper cells. Since the gp100 epitope that we used in our system is an MHC-I ($H2\text{-}D^b$) restricted (CD8) epitope, it was somewhat surprising to observe an increase in CD4 T cell frequencies. This and our previously published data[24] suggest DC activation driving homeostatic expansion of the T cell compartment.

2.4. Tumor-Infiltrating T Cell Percentages Were Significantly Increased after CpG-gp-E2 Immunization

We then examined the T cells within the TME. We found that immunization with CpG-gp-E2 nanoparticles (Groups II–IV) significantly increased CD8 T cell percentage in the TME, with Group III showing the most significant increase ($p < 0.01$) (Figure 4A). Prime and day 8 boost with CpG-gp-E2 (Group III) resulted in approximately tenfold increase in CD8 T cell percentages compared to the PBS control group. Single vaccination and day 11 boost groups (Groups II and IV) resulted in approximately fivefold increase compared to the PBS control group (Figure 4A). In these studies, all mice were sacrificed on day 15 to evaluate the splenocytes and the tumors (if existed) for T cell population, IFN-γ secretion, and PD-1 expression. By day 15, tumors were only detected in 2 of 7 mice in Group III, yielding fewer tumor data points for this group (Figure 4A,C), which is an indication of more robust antitumor responses in Group III compared to the other groups. The combined data for Group III demonstrated higher antigen-specific IFN-γ responses (Figure 2B), enhanced splenocyte CD8 T cell counts (Figure 3E), elevated CD8 T cell percentage within the TME (Figure 4A), and slower tumor growth (Figure 2C). Together, this provides evidence of a strong, CD8 T cell-driven, antitumor response.

To evaluate the potential for combination treatment of immune checkpoint inhibitor with the CpG-gp-E2 vaccine, we also assessed PD-1 expression on tumor-infiltrating CD8 T cells. Whereas the expression of PD-1 was low on CD8 T cells within the spleen (Figure 4B), CD8 T cells highly expressed PD-1 in all groups within tumor (Figure 4C). This latter observation indicated the presence of activated T cells in the TME.

2.5. Long-Term Survival Increased from 5% to 50% afterAnti-PD-1 Treatment Was Combined with the CpG-gp-E2 Vaccine

Our data suggested that double immunization with CpG-gp-E2 nanoparticle using the Group III schedule (Figure 2A) was the most effective condition in our study for eliciting antitumor cell-mediated immune responses. Additionally, we have previously shown that antitumor responses to our E2 vaccine is antigen-specific, with no response to irrelevant antigens, the E2 scaffold alone, or tumor cells that do not bear the tumor-associated antigen.[24,25] Based

on these results, we hypothesized that immunization with CpG-gp-E2 using the Group III immunization regimen to prime antigen-specificity, in combination with anti-PD-1 checkpoint inhibitor treatment to enhance immune reactivity, would increase the efficacy compared to each treatment separately. To test this hypothesis, C57BL/6 mice were inoculated with 10^4 B16-F10 cells and assigned into four different groups: anti-PD-1 alone, CpG-gp-E2 alone, combination of both anti-PD-1 and CpG-gp-E2, and PBS (control), with administration schedules summarized in Figure 5A.

2.5.1. Individual Treatment of Anti-PD-1 or CpG-gp-E2 Nanoparticle—We observed that immunization with the CpG-gp-E2 nanoparticle alone significantly increased animal survival (median survival of 36 days), compared to PBS-injected mice (median survival of 26 days; $p < 0.001$) (Figure 5B). This data demonstrates the ability of the CpG-gp-E2 nanoparticle to induce antitumor responses and increase survival times, which is consistent with our prior data for prophylactic vaccine dosing.[24] Treatment with anti-PD1 antibody alone also slightly prolonged survival time (median survival of 31 days), compared to PBS (median survival of 26 days; $p < 0.01$) (Figure 5B). Our data is consistent with prior studies demonstrating the ability of anti-PD-1 antibody (alone) to induce antitumor responses in mice,[39–41] and with clinical results showing the fraction of long term survival (≥4 years) to be about 20%.[7,8] However, although both the vaccine and anti-PD-1 treatments individually extended survival time, neither yielded significant long-term survival.

Tumor associated immune suppression has long been considered to play a major role in the limited efficacy of antitumor immunotherapies, including vaccines. With the discovery of immune checkpoints, which control T cell homeostasis and the development of drugs to block the function of these pathways, antitumor immunotherapy has been reinvigorated as the FDA has approved several immune checkpoint inhibitors for the treatment of cancer. However, even with combinations of immune checkpoint inhibition and careful patient selection, only a proportion of patients respond and delayed relapses are still observed. Thus, neither antitumor vaccines nor immune checkpoint inhibition on their own provide the efficacy that we desire.

2.5.2. Combination Treatment of Anti-PD-1 and CpG-gp-E2 Nanoparticle—The group that received the combination treatment showed a striking increase in survival compared to groups receiving CpG-gp-E2 alone ($p < 0.001$) or anti-PD1 alone ($p < 0.001$) (Figure 5). By day 53, survival was 0% for the CpG-gp-E2 alone group and approximately 5% for the anti-PD-1 alone group. In contrast, more than 50% of mice that received the combination treatment were tumor-free during the full period of the experiment (day 60) (Figure 5). We observed no obvious adverse effects in mice, as evaluated by weight loss, hair loss, and general behavior in any group.

These data indicate that the low therapeutic outcome of PD-1 inhibitor treatment is improved when the treatment is administered in combination with the E2 antigen-delivery nanoparticle. Others have also examined combining anti-PD-1 with other immunotherapies. Antonios et al. have also reported a higher survival (approximately 30% tumor-free mice) in a glioma tumor model for animals that received dendritic cell vaccination and anti-PD-1 in

combination, compared to each treatment separately.[41] Enhanced antitumor responses was also observed when anti-PD-1 antibody was administered in combination with a multipeptide vaccine.[39] Also, it has previously been reported that the addition of tumor cell lysate with poly(lactide-*co*-glycolide) or TEGVAX cancer vaccine to anti-PD-1 resulted in effective antitumor responses in the B16-F10 tumor model.[40,42] In the poly(lactide-*co*-glycolide) study, immune checkpoint inhibition was initiated first, followed by immunization later, with the stated rationale that this was likely to be the clinical strategy given the first line therapy for immune checkpoint inhibitors.[42] It is not clear that the addition of immunization to pre-existing immune checkpoint inhibition is better than addition of immune checkpoint inhibition to prior antitumor immunization, or with an extended immunization schedule analogous to a study performed by Ali et al.[42] We would argue that priming or educating the immune system before applying immune checkpoint inhibition is more consistent with our current understanding of immune system homeostasis. Regardless, our data, together with others and existing clinical results, confirm that combination approaches to increase immune activation are needed to increase the antitumor response generated from anti-PD-1 therapy and extend lifespan.

2.5.3. Impact of Treatments on the TME—Tumor cells are known to escape immune responses by MHC-I downregulation, antigen mutation or downregulation, and/or programmed death-ligand 1 (PD-L1) upregulation.[43] Throughout the combination therapy study, we isolated and examined tumors for MHC-I, gp100, and PD-L1 expression ($n = 4$ per group selected from those animals who developed tumors). Our data indicate low MHC-I expression in tumor cells isolated from all groups (Figure 6A). Low expression of MHC-I in a poorly immunogenic tumor model (e.g., B16-F10) is not surprising, as other studies have also detected low expression of MHC-I on B16 melanoma cells.[44,45]

Interestingly, immunization with CpG-gp-E2 nanoparticles alone, or in combination with anti-PD-1, significantly decreased the levels of MHC-I expression compared to the control group (Figure 6A). This observation implies that tumor cells downregulated the levels of MHC-I expression to evade the higher/stronger specific CD8 T cell responses in the TME. Furthermore, we did not detect a significant decrease in gp100-antigen expression in any of the groups (Figure 6B), suggesting that tumor escape is likely not due to changes in antigen expression levels on the tumor cells. Combination treatment of anti-PD-1 with CpG-gpE2 nanoparticle did, however, result in PD-L1 downregulation (Figure 6C), possibly to attenuate the anti-PD-1 therapy and produce resistance. PD-L1 promoter methylation and PD-L1 downregulation were previously described in a nonsmall cell lung cancer (NSCLC) murine model, in agreement with our findings.[46] Adaptive resistance to PD-1 treatment may also be associated with upregulation of alternative immune checkpoints such as T-cell immunoglobulin mucin-3 (TIM-3),[47] but this was not examined in our investigation. Furthermore, our finding of lower MHC-I expression in the tumors from the CpG-gp-E2 and combined groups implies that tumor cells with decreased MHC-I expression were selected by the robust elicited antigen-specific immune response.

In prior studies reporting the combination of antitumor vaccines and immune checkpoint inhibition, slower tumor growth and extended survival rates were also observed for combination treatment compared to immune checkpoint therapy alone.[48,49] However, those

strategies did not yield sufficient activity to result in cures of poorly immunogenic tumors (e.g., B16-F10). Thus, we believe our data support the exceptional utility of our nonviral E2 protein nanoparticle platform when combined with immune checkpoint blockade.

2.6. Evidence of Durable Response Is Observed in Surviving Mice of Combined Therapy

One significant effect of cancer vaccines is the potential to induce a durable/memory response that can be expanded on recall and protect individuals against recurrence. To test for this, we rechallenged the tumor-free mice from the combined therapy group that survived (Figure 5B) with 10^4 B16-F10 cells. Mice did not receive any further nanoparticle immunization and anti-PD1 therapy, and age-matched mice having received no prior treatments (naive) served as the control. A significant increase was observed in survival time of rechallenged mice from the combined group (median 30 days vs 18 days for the control) ($p < 0.01$) (Figure 7). These data support the development of long-lasting antitumor response due to the vaccine and checkpoint inhibition combination therapy. Induction of durable responses has also been observed by others, for example, after administration of CpG and ovalbumin-conjugated nano particles.[50] Karyampudi et al. also observed accumulation of memory T cells following combination therapy of a multipeptide cancer vaccine and antiPD-1 antibody.[39]

3. Conclusions

This work shows the advantage of combining anti-PD-1 (which enhances overall immune response) with E2 antigen delivery nanoparticles (with prime antigen-specificity) as an effective immunotherapy strategy in the poorly immunogenic B16-F10 syngeneic melanoma model. The approach augmented the CD8 T cell population, resulted in an effective long-term survival rate, and elicited an efficient and durable immune response. To our knowledge, we are the first group to report the synergistic effects of combination therapy of anti-PD-1 with a protein-based, antigen-delivery nanoparticle vaccine, an approach that could be promising for enhancing cancer treatment efficacies. These data together support the exceptional utility of our E2 nanoparticle-based vaccine, especially when combined with immune checkpoint blockade.

4. Experimental Section

Cell Culture:

Reagents were from Fisher Scientific unless otherwise noted. Complete RPMI for splenocytes comprised RPMI 1640 (Mediatech) with 10% heat-inactivated FBS (Hyclone), 1×10^{-3} m sodium pyruvate (Hyclone), 100 μg mL^{-1} of streptomycin (Hyclone), 0.1×10^{-3} m nonessential amino acids (Lonza), 2×10^{-3} m l-glutamine (Lonza), and 100 units mL^{-1} penicillin. B16-F10, a murine melanoma cell line, was purchased from ATCC and cultured in DMEM supplemented with 10% FBS. Cellswere incubatedat37 °C,under 5% CO_2, andwere passaged2–3 times a week.

E2 Nanoparticle Purification, Conjugation, and Characterization:

Expression Purification and characterization of the D381C form of the E2 protein nanoparticle vaccine (abbreviated "E2" in this study) were performed as previously described.[22,24,25] In summary, *Escherichia coli* strain BL21(DE3) containing the E2 gene was cultured in Luria-Bertani medium containing ampicillin, E2 expression was induced with IPTG, and cells were harvested and lysed. The E2 nanoparticle was purified by heat precipitation, followed by FPLC purification with HiPrep Q Sepharose anion exchange and Superose 6 size exclusion columns.[26] Nanoparticle characterization included SDS-PAGE, dynamic light scattering, transmission electron microscopy, and zeta potential.[25] Lipopolysaccharide was removed using Triton X-114 (Sigma) extraction, and endotoxin levels were evaluated using an LAL ToxinSensor kit (Genscript).[22]

Nanoparticle vaccines abbreviated as "CpG-gp-E2" denoted E2 nanoparticles that were conjugated to a gp100 peptide epitope on the particle surface and CpG within the internal cavity. Specifically, 5′ benzaldehyde-modified CpG 1826 [5′-tccatgacgttcctgacgtt-3′] with a phosphorothioated backbone was synthesized by Trilink. This CpG 1826 was attached to the cysteines in the internal cavity of E2 nanoparticles using a *N*-*β*-maleimidopropionic acid hydrazide (BMPH) linker. TCEP-reduced peptides with N-terminal cysteines were conjugated to the lysines on the surface of the E2 nanoparticle with a sulfo-SMCC linker, as previously described.[24,25] The number of conjugated CpG molecules was determined previously to average 22 CpG molecules per E2 particle and was estimated with intensity analysis in ImageJ software, using standardized concentrations.[22]

The $gp100_{25–33}$ antigen, CKVPRNQDWL, containing a well-described H2-D^b restricted epitope from human gp100 that elicits cytotoxic T lymphocyte (CTL) responses to murine gp100, was synthesized by Genemed Synthesis.[51] For peptide attachment, peptide was added to E2 functionalized with sulfo-SMCC linker at a tenfold excess to E2 monomer. The negative control consisted of water instead of sulfo-SMCC (solvent for sulfo-SMCC) combined with E2 in the initial reaction step. For measurement of peptide conjugation ratios, gp100-conjugated E2 (gp-E2) was analyzed by high performance liquid chromatography (HPLC, Shimadzu) with a Zorbex C18 column using a water:acetonitrile gradient. Mixtures were examined by HPLC, and the remaining unconjugated peptide was quantified with a standard curve of free cysteine-terminated gp100 peptide as previously described.[24] The difference between gp-E2 and negative control reactions determined the number of conjugated peptides per nanoparticle.[24]

Tumor Challenge:

All animal studies were carried out in accordance with protocols approved by the Institute for Animal Care and Use Committee (IACUC) at the University of California, Irvine. Female C57BL/6 mice (6 to 8 weeks) were obtained from Jackson Laboratory. B16-F10 melanoma cells were subcutaneously inoculated in the right flank, and tumor size was measured at least every other day with a caliper. For the immunization schedule study, mice were challenged with 10^5 B16-F10 cells. For the combination study, the mice inoculated with 10^4 B16-F10 cells to allow for sufficient time to complete the treatments and to monitor the mice for long-term survival. Tumor volume was calculated as (0.5 × shortest diameter^2 ×

longest diameter). In studies to establish optimal E2 immunization schedules, mice were euthanized on day 15. For the combination and rechallenge studies, mice were euthanized when tumors reached 1.5 cm in diameter.

Treatments:

All immunizations with CpG-gp-E2 nanoparticle (in 120 μL LPS-free PBS) were injected subcutaneously at the base of the tail. Different immunization schedules were tested in this study and are summarized in Figures 2A and 5A. Anti-PD-1 antibody (Bio X Cell, clone [RPM1–14]) was administered by intraperitoneal (IP) injection. Mice received 5 injections of 100 μg anti-PD-1 (in 200 μL PBS) every 3 days starting at day 9, unless mice were euthanized earlier because of tumor size (2 mice from anti-PD-1 and 2 from the combined group received only 3 injections). All treatments were administered starting 24 h after administration of the B16-F10 tumor inoculation, a timing consistent with other therapeutic studies, for example, by Allison et al.[52] Surviving mice were evaluated for a durable antitumor response by tumor rechallenge, with untreated naïve mice as the positive control for tumor establishment.

IFN-γ:

ELISpots were performed using the Ready-Set-Go kit for IFN-γ (eBioscience). Single-cell suspensions in RPMI were prepared from isolated spleens and 10^6 cells per well were added to PVDF ELISpot plates that were precoated with antimouse IFN-γ antibody. Cells were incubated with either 10 μg mL^{-1} of the relevant peptide or an irrelevant peptide (SIINFEKL) for 24 h at 37 °C. Unstimulated cells in RPMI served as a negative control. Positive controls contained 2% PHA-M (Gibco). IFN-γ spots were developed following the manufacturer's protocol. Plates were scanned and quantified using an Immunospot ELISpot reader and analysis software (Cellular Technology).

Flow Cytometry:

Single-cell suspensions from individual tumors and spleens were prepared to examine their resident cell types and cell surface markers. Red blood cells were depleted with ACK lysing buffer. Cells were washed twice in PBS and counted on a hemocytometer. Cells were stained with primary antibodies or appropriate isotype controls in PBS + 1% BSA (FACS buffer) for 30 min on ice, followed by 2 washes with FACS buffer. For gp100, cells were stained with an unconjugated primary antibody, washed twice with FACS buffer, and incubated with the secondary antibody for 30 min, followed by 2 washes. Flow cytometry was performed by a NovoCyte flow cytometer and analyzed by NovoExpress software (ACEA Biosciences). For analysis, a typical forward-side scatter gate was set to exclude dead cells and aggregates. Antibodies were from Life Technologies, unless otherwise noted. These antibodies included anti-CD8 (clone, 536.7), anti-CD4 (Gk1.5), anti-CD3 (145–2C11), anti-PD-1 (J43), anti-MHC-I (AF6–88.5.5.3), anti-PD-L1 (MIH5), and antimelanoma gp100 (EP4863(2), Abcam), with the secondary antibody of goat antirabbit IgG (Alexa Fluor 488). Rat IgG2a, k (RTK2758), rat IgG2b, k (RTK4530), Armenian hamster IgG (HTK888), and mouse IgG2a, k (eBM2a) were used as isotype controls.

Statistical Analysis:

Data were presented as mean ± standard deviation for particle characterization of at least 3 independent experiments. Data for different nanoparticle immunization regimens were presented as mean ± standard error of the mean (S.E.M.); results represented pooled data from multiple independent experiments ($n_{total} = 7$). Statistical significance across groups was determined by one-way ANOVA followed by post-hoc Tukey's test. Statistical analyses of survival curves in the combination study ($n_{total} = 15$) and the rechallenge study ($n_{total} = 7$) were determined by log-rank (Mantel–Cox); results represented pooled data from multiple independent experiments. Data for expression of tumor cell surface markers (e.g., MHC-I) were presented as mean ± S.E.M. ($n$total = 4); statistical significance was determined by one-way ANOVA together with post-hoc Tukey's test across all groups. In all cases, p-values less than 0.05 were considered statistically significant. Statistical analyses were performed using GraphPad Prism in all cases, unless otherwise noted.

Supplementary Material

Refer to Web version on PubMed Central for supplementary material.

Acknowledgements

Flow cytometry was carried out at the UCI Flow Cytometry Core Facility in the Institute for Immunology. This work was supported by the National Institute of Biomedical Imaging and Bioengineering (R21EB017995 and 1R01EB027797-01) and the National Cancer Institute (P30CA062203) of the National Institutes of Health.

References

[1]. Pardoll DM, Nat. Rev. Cancer 2012, 12, 252. [PubMed: 22437870]

[2]. Villadolid J, Amin A, Transl. Lung Cancer Res 2015, 4, 560. [PubMed: 26629425]

[3]. Fife BT, Bluestone JA, Immunol. Rev 2008, 224, 166. [PubMed: 18759926]

[4]. Francisco LM, Sage PT, Sharpe AH, Immunol. Rev 2010, 236, 219. [PubMed: 20636820]

[5]. Lipson EJ, Drake CG, Clin. Cancer Res 2011, 17, 6958. [PubMed: 21900389]

[6]. Larkin J, Chiarion-Sileni V, Gonzalez R, Grob JJ, Cowey CL, Lao CD, Schadendorf D, Dummer R, Smylie M, Rutkowski P, Ferrucci PF, Hill A, Wagstaff J, Carlino MS, Haanen JB, Maio M, Marquez-Rodas I, McArthur GA, Ascierto PA, Long GV, Callahan MK, Postow MA, Grossmann K, Sznol M, Dreno B, Bastholt L, Yang A, Rollin LM, Horak C, Hodi FS, Wolchok JD, N. Engl. J. Med 2015, 373, 23. [PubMed: 26027431]

[7]. Postow MA, Callahan MK, Wolchok JD, J. Clin. Oncol 2015, 33, 1974. [PubMed: 25605845]

[8]. Maio M, Grob JJ, Aamdal S, Bondarenko I, Robert C, Thomas L, Garbe C, Chiarion-Sileni V, Testori A, Chen TT, Tschaika M, Wolchok JD, J. Clin. Oncol 2015, 33, 1191. [PubMed: 25713437]

[9]. Rogiers A, Boekhout A, Schwarze JK, Awada G, Blank CU, Neyns B, J. Oncol 2019, 2019, 5269062.

[10]. Ruan H, Bu L, Hu Q, Cheng H, Lu W, Gu Z, Adv. Healthcare Mater 2019, 8, 1801099.

[11]. Sato-Kaneko F, Yao S, Ahmadi A, Zhang SS, Hosoya T, Kaneda MM, Varner JA, Pu M, Messer KS, Guiducci C, Coffman RL, Kitaura K, Matsutani T, Suzuki R, Carson DA, Hayashi T, Cohen EEW, JCI Insight 2017, 2, e93397.

[12]. Llopiz D, Ruiz M, Villanueva L, Iglesias T, Silva L, Egea J, Lasarte JJ, Pivette P, Trochon V, Bérangère J, Graham V, Sangro B, Sarobe P, Cancer Immunol. Immunother 2019, 68, 379. [PubMed: 30547218]

[13]. Wong KK, Li WWA, Mooney DJ, Dranoff G, Adv. Immunol 2016, 130, 191. [PubMed: 26923002]

[14]. Zhao L, Seth A, Wibowo N, Zhao C, Mitter N, Yu C, Middelberg APJ, Vaccine 2014, 32, 327. [PubMed: 24295808]

[15]. Neek M, Il Kim T, Wang SW, Nanomedicine 2019, 15, 164. [PubMed: 30291897]

[16]. Park YM, Lee SJ, Kim YS, Lee MH, Cha GS, Jung ID, Kang TH, Han HD, Immune Network 2013, 13, 177. [PubMed: 24198742]

[17]. Fan Y, Moon JJ, Vaccines 2015, 3, 662. [PubMed: 26350600]

[18]. Peek LJ, Middaugh CR, Berkland C, Adv. Drug Delivery Rev 2008, 60, 915.

[19]. Bachmann MF, Jennings GT, Nat. Rev. Immunol 2010, 10, 787. [PubMed: 20948547]

[20]. Molino NM, Bilotkach K, Fraser DA, Ren D, Wang SW, Biomacromolecules 2012, 13, 974. [PubMed: 22416762]

[21]. Ren D, Dalmau M, Randall A, Shindel MM, Baldi P, Wang SW, Adv. Funct. Mater 2012, 22, 3170. [PubMed: 23526705]

[22]. Molino NM, Anderson AKL, Nelson EL, Wang SW, ACS Nano 2013, 7, 9743. [PubMed: 24090491]

[23]. Ren D, Kratz F, Wang SW, Small 2011, 7, 1051. [PubMed: 21456086]

[24]. Molino NM, Neek M, Anne J, Nelson EL, Wang SW, Biomaterials 2016, 86, 83. [PubMed: 26894870]

[25]. Neek M, Tucker JA, Il Kim T, Molino NM, Nelson EL, Wang SW, Biomaterials 2018, 156, 194. [PubMed: 29202325]

[26]. Dalmau M, Lim S, Chen HC, Ruiz C, Wang SW, Biotechnol. Bioeng 2008, 101, 654. [PubMed: 18814295]

[27]. Molino NM, Neek M, Tucker JA, Nelson EL, Wang SW, ACS Biomater. Sci. Eng 2017, 3, 496. [PubMed: 28989957]

[28]. Besser MJ, Shapira-Frommer R, Itzhaki O, Treves AJ, Zippel DB, Levy D, Kubi A, Shoshani N, Zikich D, Ohayon Y, Ohayon D, Shalmon B, Markel G, Yerushalmi R, Apter S, Ben-Nun A, Ben-Ami E, Shimoni A, Nagler A, Schachter J, Curigliano G, Perez EA, Curti BD, Kovacsovics-Bankowski M, Morris N, Walker E, Chisholm L, Floyd K, Walker J, Gonzalez I, et al., Cancer Res. 2013, 25, 5.

[29]. Milone MC, Bhoj VG, Mol. Ther.–Methods Clin. Dev 2018, 8, 210. [PubMed: 29552577]

[30]. Liston A, Gray DHD, Nat. Rev. Immunol 2014, 14, 154. [PubMed: 24481337]

[31]. Josefowicz SZ, Lu L, Rudensky AY, Annu. Rev. Immunol 2012, 30, 531. [PubMed: 22224781]

[32]. Hamdy S, Elamanchili P, Alshamsan A, Molavi O, Satou T, Samuel J, J. Biomed. Mater. Res 2007, 81A, 652.

[33]. Wang X, Chen X, Manjili MH, Repasky E, Henderson R, Subjeck JR, Cancer Res. 2003, 63, 2553. [PubMed: 12750279]

[34]. Xu Z, Ramishetti S, Tseng YC, Guo S, Wang Y, Huang L, J. Controlled Release 2013, 172, 259.

[35]. Zhang Z, Tongchusak S, Mizukami Y, Kang YJ, Ioji T, Touma M, Reinhold B, Keskin DB, Reinherz EL, Sasada T, Biomaterials 2011, 32, 3666. [PubMed: 21345488]

[36]. Mahmoud SMA, Paish EC, Powe DG, Macmillan RD, Grainge MJ, J. Clin. Oncol 2011, 29, 1949. [PubMed: 21483002]

[37]. Andersen MH, Pedersen L, Capeller B, Bro E, Becker C, Straten P, Cancer Res. 2001, 1, 5964.

[38]. Bourquin C, Anz D, Zwiorek K, Lanz AL, Fuchs S, Weigel S, Wurzenberger C, von der Borch P, Golic M, Moder S, Winter G, Coester C, Endres S, J. Immunol 2008, 181, 2990. [PubMed: 18713969]

[39]. Karyampudi L, Lamichhane P, Scheid AD, Kalli KR, Shreeder B, Krempski JW, Behrens MD, Knutson KL, Cancer Res. 2014, 74, 2974. [PubMed: 24728077]

[40]. Fu J, Malm IJ, Kadayakkara DK, Levitsky H, Pardoll D, Kim YJ, Cancer Res. 2014, 74, 4042. [PubMed: 24812273]

[41]. Antonios JP, Soto H, Everson RG, Orpilla J, Moughon D, Shin N, Sedighim S, Yong WH, Li G, Cloughesy TF, Liau LM, Prins RM, JCI Insight 2016, 1, e87059.

[42]. Ali OA, Lewin SA, Dranoff G, Mooney DJ, Cancer Immunol. Res 2016, 4, 95. [PubMed: 26669718]

[43]. Rabinovich GA, Gabrilovich D, Sotomayor EM, Annu. Rev. Immunol 2007, 25, 267. [PubMed: 17134371]

[44]. Riond J, Rodriguez S, Nicolau ML, Saati TA, Gairin JE, Cancer Immun. 2009, 9, 10. [PubMed: 19877577]

[45]. Mansour M, Pohajdak B, Kast WM, Fuentes-Ortega A, KoretsSmith E, Weir GM, Brown RG, Daftarian P, J. Transl. Med 2007, 5, 20. [PubMed: 17451606]

[46]. Zhang Y, Xiang C, Wang Y, Duan Y, Liu C, Oncotarget 2017, 8, 101535.

[47]. Koyama S, Akbay EA, Li YY, Herter-sprie GS, Buczkowski KA, Richards WG, Gandhi L, Redig AJ, Rodig SJ, Asahina H, Jones RE, Kulkarni MM, Kuraguchi M, Palakurthi S, Fecci PE, Johnson BE, Janne PA, Engelman JA, Gangadharan SP, Costa DB, Freeman GJ, Bueno R, Hodi FS, Dranoff G, Wong K, Hammerman PS, Nat. Commun 2016, 7, 10501. [PubMed: 26883990]

[48]. Duperret EK, Wise MC, Trautz A, Villarreal DO, Ferraro B, Walters J, Yan J, Khan A, Masteller E, Humeau L, Weiner DB, Mol. Ther 2018, 26, 435. [PubMed: 29249395]

[49]. Takeda Y, Yoshida S, Takashima K, Shime H, Seya T, Matsumoto M, Cancer Sci. 2018, 109, 2119. [PubMed: 29791768]

[50]. Titta A, Ballester M, Julier Z, Nembrini C, Jeanbart L, van der Vlies AJ, Swartz MA, Hubbell JA, Proc. Natl. Acad. Sci. USA 2013, 110, 19902. [PubMed: 24248387]

[51]. Overwijk BWW, Tsung A, Irvine KR, Parkhurst MR, Goletz TJ, Tsung K, Carroll MW, Liu C, Moss B, Rosenberg SA, Restifo NP, J. Exp. Med 1998, 188, 277. [PubMed: 9670040]

[52]. van Elsas A, Hurwitz AA, Allison JP, J. Exp. Med 1999, 190, 355. [PubMed: 10430624]

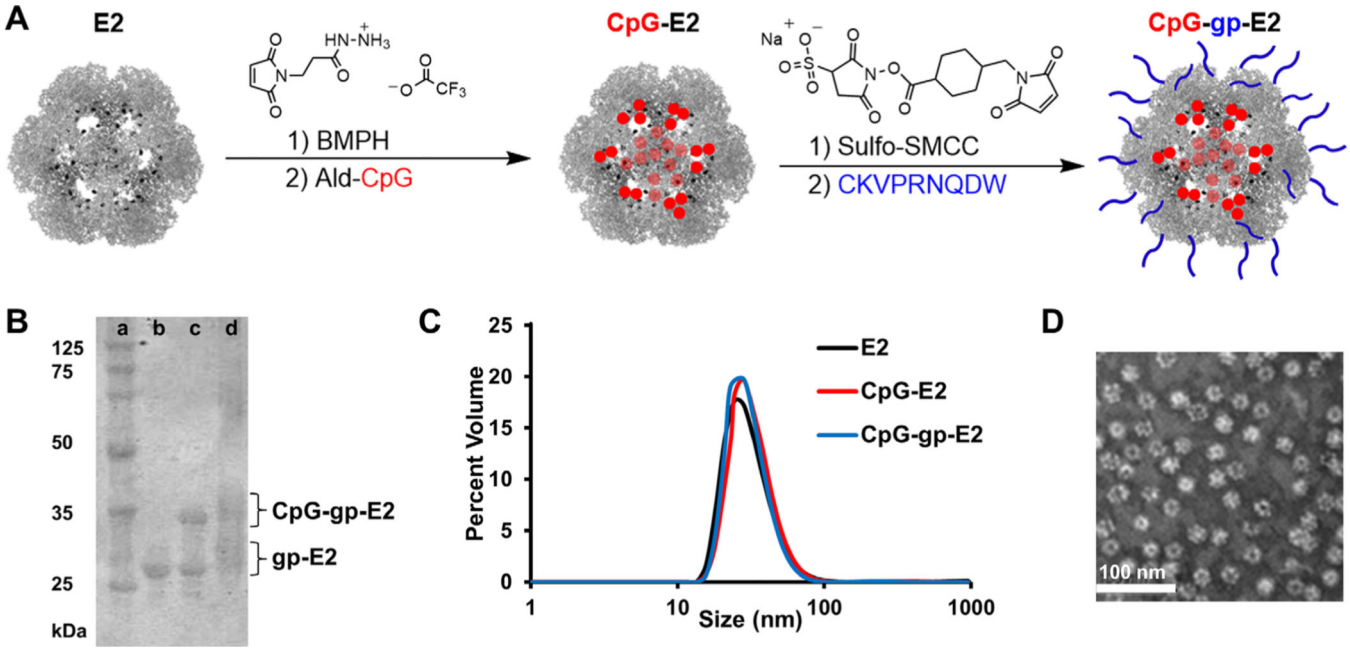

Figure 1.

Characterization of functionalized nanoparticles. A) Schematic of conjugation strategy to synthesize CpG-gp-E2. The internal cysteines (black) of the E2 protein nanoparticle are conjugated to aldehyde-modified CpG (red) via a BMPH linker. Surface lysines on E2 are reacted with a sulfo-SMCC linker, and then cysteine-modified gp100 peptide (blue). B) SDS-PAGE shows conjugation of CpG and gp100 to E2 nanoparticles. Lanes: a) protein ladder, b) E2 only, c) conjugation of CpG to E2 (CpG-E2), and d) conjugation of CpG and gp100 to E2 (two broad bands indicative of gp-E2 and CpG-gp-E2 are highlighted). C) DLS reveals nanoparticle sizes of ≈30 nm for all E2-based nanoparticles. D) TEM image of CpG-gp-E2 confirms intact nanoparticles (scale bar = 100 nm).

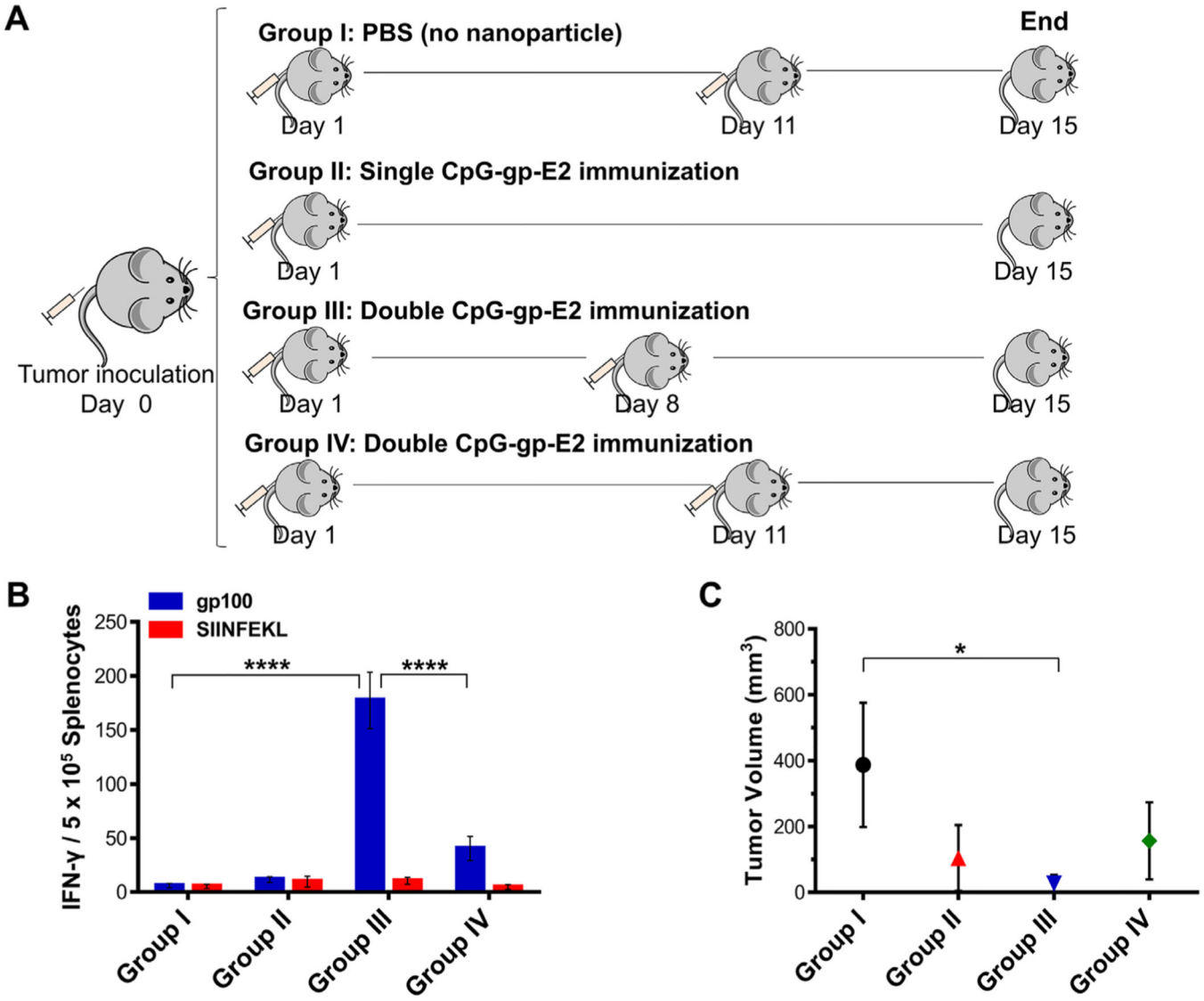

Figure 2.

ELISpot analysis of splenocytes and tumor size data on day 15. A) Schematic of different immunization schedules (Groups I–IV). B) Summary of ELISpot data evaluating antigen-specific IFN-γ secretion. C57BL/6 mice were immunized with different regimens (Groups I–IV), and splenocytes were pulsed ex vivo in the presence of relevant peptide (gp100) or irrelevant peptide (SIINFEKL) and analyzed for IFN-γ secretion (n_{total} = 7 per group). C) Average tumor size on day 15. Double immunization with CpG-gp-E2 (Group III) significantly decreased the tumor growth compared to other groups. Tumor volumes of Groups I, II, and IV are not significantly different ($p > 0.05$). Data represent mean ± S.E.M. (n_{total} = 7 per group). Statistical significance was determined by one-way ANOVA followed by post-hoc Tukey's test (*$p < 0.05$; ****$p < 0.0001$).

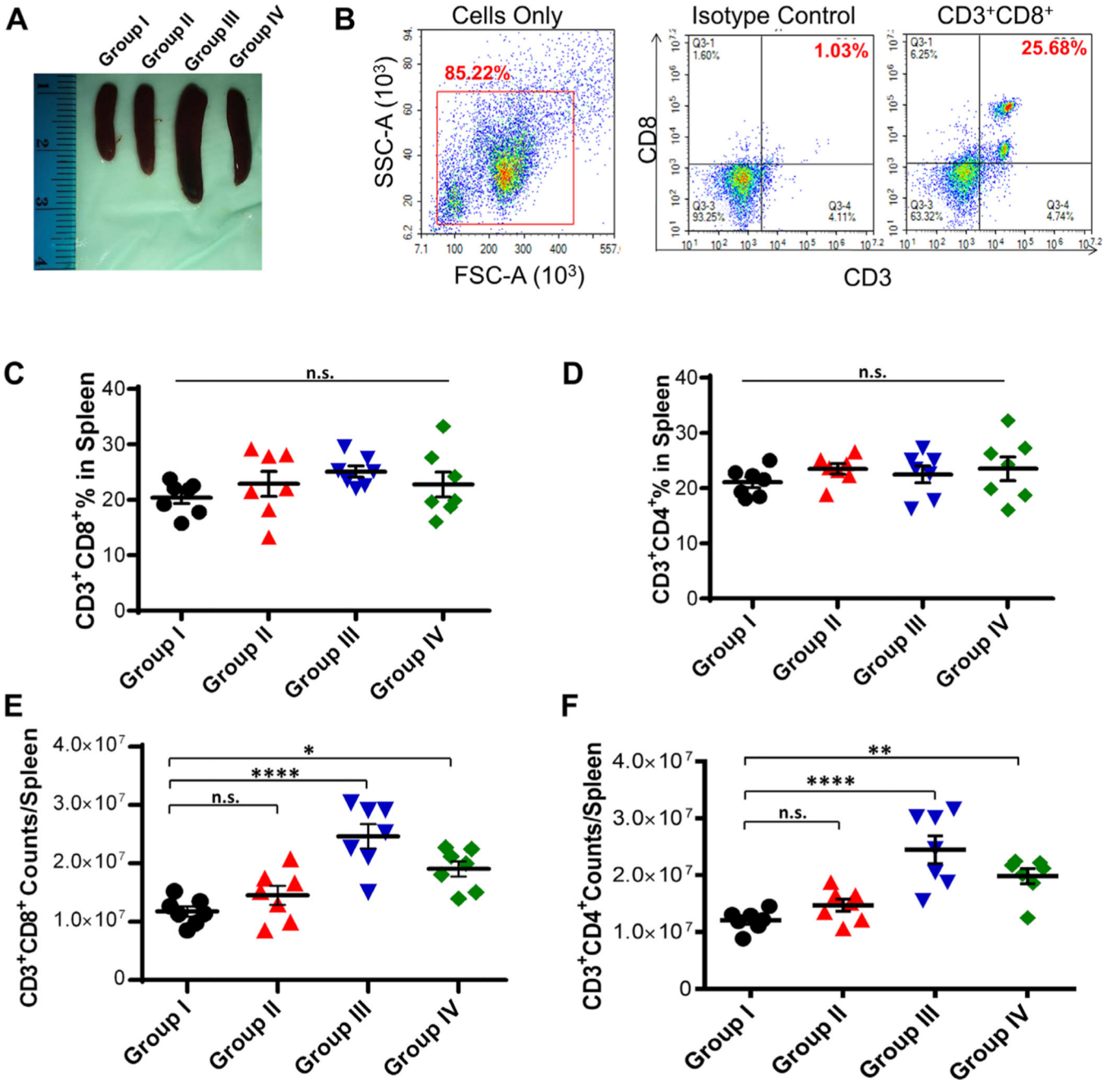

Figure 3.

T cell population in splenocytes. C57BL/6 mice inoculated with B16-F10 received different nanoparticle immunizations. A) Representative spleens isolated from different groups. B) Representative flow cytometry data of CD8 T cells from Group III. C) CD8 T cell percentages in splenocytes; no statistical differences were observed between the different groups. D) CD4 T cell percentages in splenocytes; no statistical differences were observed. E) CD8 T cell count within splenocytes. F) CD 4 T cell count in splenocytes. Data represent mean ± S.E.M. (n_{total} = 7 per group). Statistical significance was determined by one-way

ANOVA followed by post-hoc Tukey's test. *$p < 0.05$; **$p < 0.01$; ****$p < 0.0001$; n.s. = no significance.

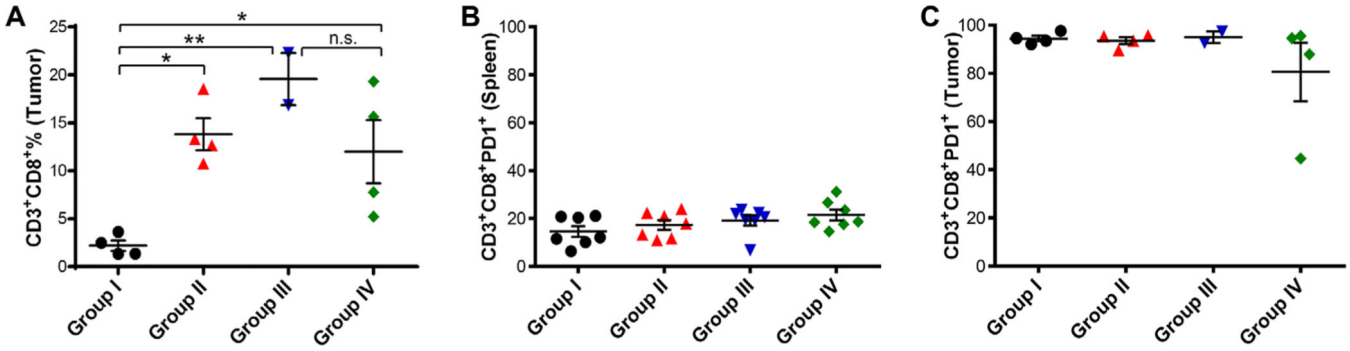

Figure 4.

CD8 T cells in spleen and tumor microenvironment. A) CD8 T cell percentage in the tumor microenvironment (n_{total} = 4 per group), except for Group III of which only 2 individuals developed tumors. B) PD-1 expression of CD8 T cells within spleen (n_{total} = 7). C) PD-1 expression of CD8 T cells within tumor (n_{total} = 4 per group), except for Group III of which only 2 individuals developed tumors. C57BL/6 mice were challenged with B16-F10 and received different regimens of CpG-gp-E2 immunization. Data represent mean ± S.E.M. Statistical significance was determined by one-way ANOVA followed by post-hoc Tukey's test. *$p < 0.05$; **$p < 0.01$.

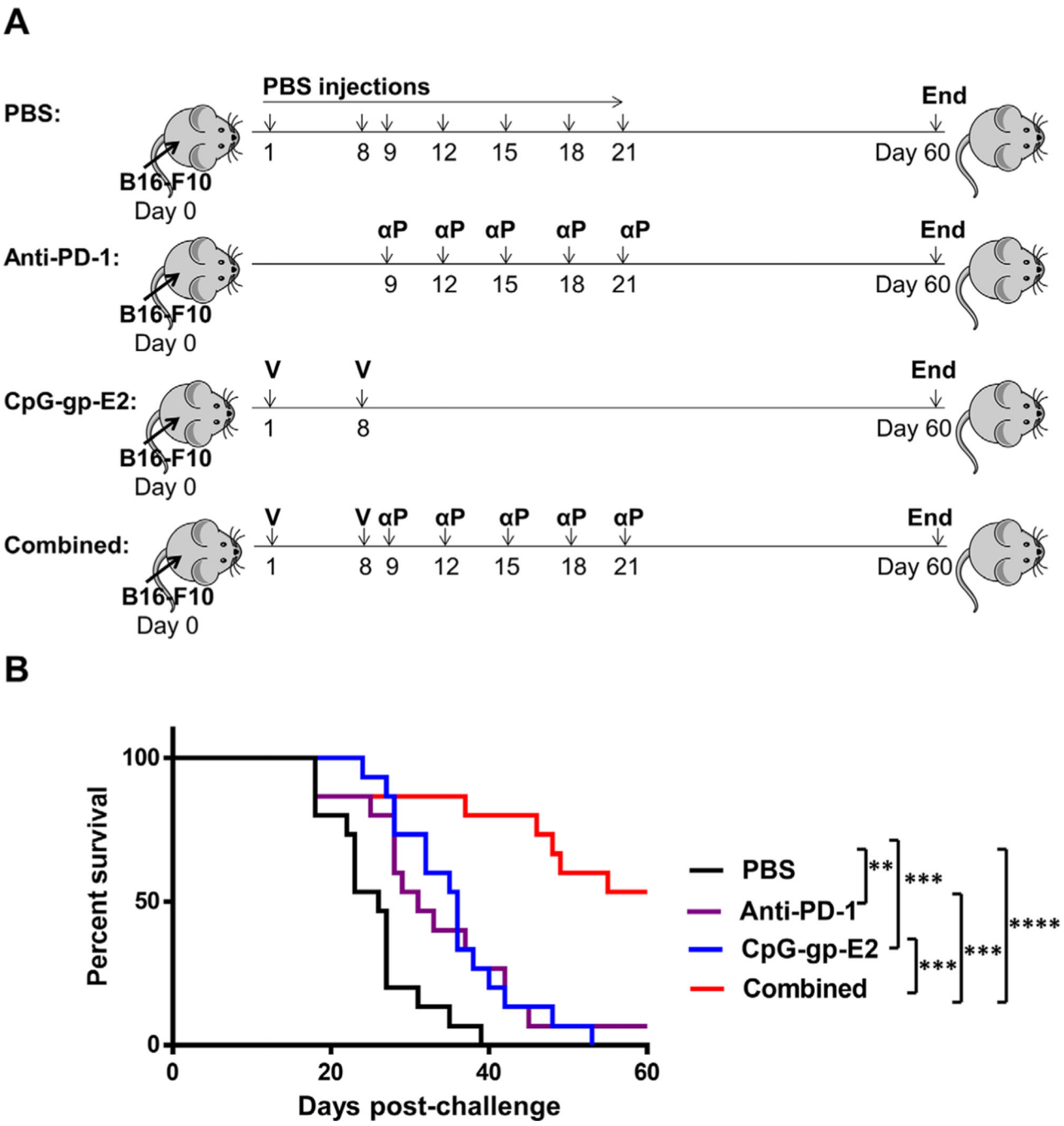

Figure 5.

Survival results for combination therapy. A) Schematic of anti-PD-1 and CpG-gp-E2 administration regimens of the different groups (V = CpGgp-E2 vaccine; *α*P = anti-PD-1). B) Kaplan–Meier survival curves of tumor-challenge study. Combination of CpG-gp-E2 nanoparticle immunization and anti-PD-1 treatment increased survival time compared to each immunization/treatment separately. C57BL/6 mice were inoculated with B16-F10 cells, followed by treatment with control (PBS), checkpoint inhibitor alone (anti-PD-1), nanoparticle vaccine alone (CpG-gp-E2), or combination of antiPD-1 with CpG-gp-E2

(combined) (n_{total} = 15). Statistical significance was determined by log-rank (Mantel–Cox) analysis. **$p < 0.01$; ***$p < 0.001$; ****$p < 0.0001$.

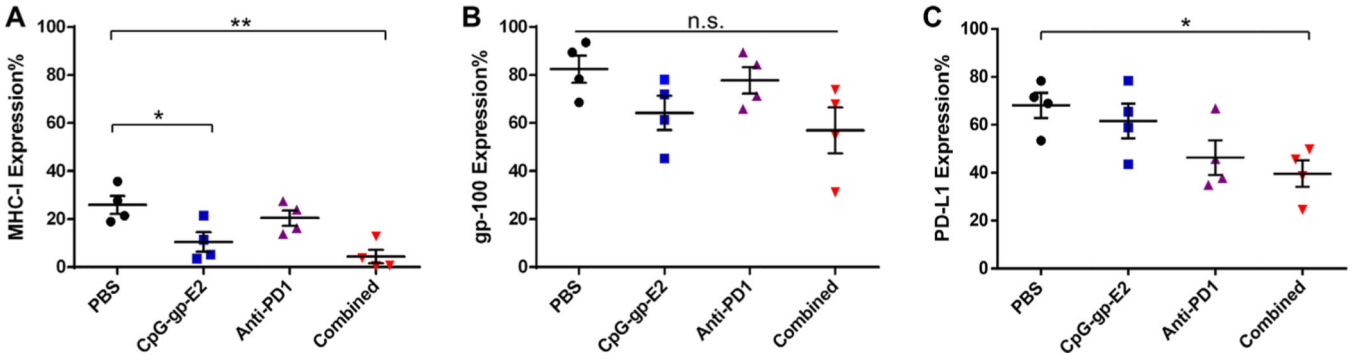

Figure 6.

Expression of A) MHC-I, B) gp100, and C) PD-L1 on tumor cells after treatment. Throughout the combination study, tumors from mice were isolated and checked for MHC-I, gp100, and PD-L1. Expression was evaluated using flow cytometry on B16-F10 tumor cells after PBS (control), CpGgp-E2, anti-PD1, and the combined treatments. Data represent mean ± S.E.M. (n_{total} = 4 per group). Statistical significance was determined by one-way ANOVA followed by post-hoc Tukey's test. *$p < 0.05$; **$p < 0.01$.

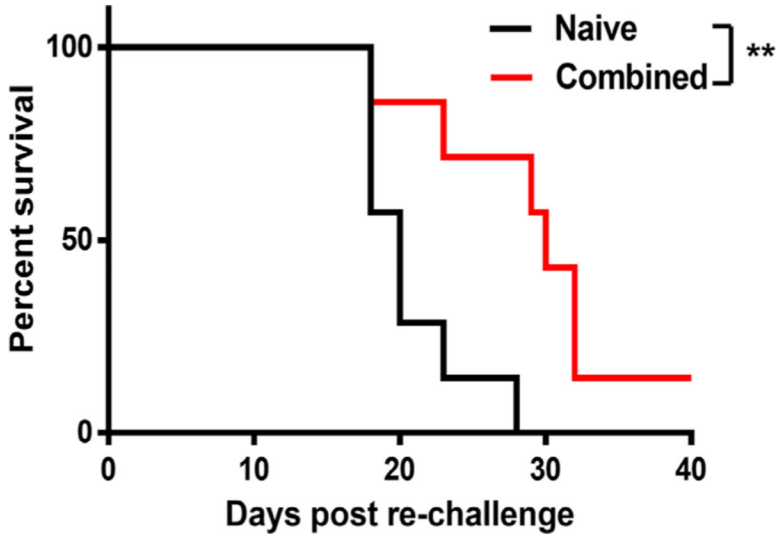

Figure 7.

Survival curve after tumor reinoculation of the combined (antiPD-1 + CpG-gp-E2) group. Tumor-free mice from combination study were reinoculated with B16-F10 cells, with no further treatments. Combination of CpG-gp-E2 nanoparticle immunization and anti-PD-1 treatment increased the survival time upon tumor rechallenge ($n_{total} = 7$). Statistical significance was determined by log-rank (Mantel–Cox)analysis. $^{**}p < 0.01$.